Theory of transient self-focusing of a CO_2 laser pulse in a cold dense plasma

A. Schmitt and R. S. B. Ong
Departments of Nuclear and Aerospace Engineering, University of Michigan, Ann Arbor, Michigan MI 48109

(Received 29 July 1982; accepted for publication 7 December 1982)

The self-focusing of laser pulses in a plasma is theoretically investigated for the situation in which the refractive index change is not in equilibrium with the pulse. In particular, the analysis models a CO_2 laser–plasma interaction experiment in which the ponderomotive and thermal conduction dominated mechanisms of self-focusing are dominant. The moment method and the Gaussian shape ansatz are used to describe the laser pulse propagation. Threshold powers are derived for the transient self-focusing process, which reveals that self-focusing can occur even for times much less than the characteristic dielectric relaxation time. Because of the behavior of the pulse heating, thermal conduction dominated self-focusing is inherently a transient phenomenon without a true steady state limit. The governing equations are also numerically solved, revealing the existence of ion acoustic waves created by the action of moving focal spots. These transversely propagating waves may be responsible for breakup or filamentation of the laser pulse.

PACS numbers: 42.65.Jx, 52.40.Db, 52.35.Mw

I. INTRODUCTION

The nonlinear interaction of laser light with plasmas has been of intense interest recently, mainly because of its relevance to laser fusion research. One of the simplest nonlinear effects that can occur for a laser pulse with transverse variations is the self-focusing or filamentation instability. The self-focusing of light in matter has long been studied, as it was one of the earliest nonlinear optical effects to be observed.[1] Since then it has been investigated in connection with the interaction of laser light with many types of solids, liquids, and gases.[2] In plasmas, self-focusing theory has applications in ionospheric propagation of waves and the interaction of pulsar radiation in space plasmas as well as in laser fusion research.

In laser fusion applications, the self-focusing or filamentation of the light can destroy the symmetry of illumination needed for proper implosion of the target, as it reduces the scale length and increases the magnitude of the transverse beam nonuniformities. Because of the complex electromagnetic character of the plasma, there are many consequences to this effect. The higher intensities achieved in the focused spots can reduce the thresholds needed to drive other nonlinear processes, such as parametric instabilities. In this way, it has been shown that the self-focused filaments can alter the energy deposition profile in the axial direction by spreading the absorption and plasma heating over a wider range of densities.[3] The presence of such filaments can thus cause a major change in the character and magnitude of the laser–plasma interactions.

Because of the profound effect on the character of the interaction, self-focusing in plasmas has been the subject of several previous studies. Kaw, Schmidt, and Wilcox[4] first analyzed the plasma filamentation instability with a perturbation approach, and then investigated the nonlinear self-trapped state in a planar configuration. The stability of these solutions was successively analyzed, and it was found that such filaments can be unstable to kink,[5] necking,[6] and modulational type[7] perturbations.

The steady state propagation of cylindrical beams in plasma under the influence of the ponderomotive force has been analzed by Max[8] and Sodha *et al.*,[9] using the paraxial ray formalism. In recent years, two other approaches, the moment method[10] and the variational method,[11] have been shown to be more accurate than the paraxial ray method when compared to more complete numerical analyses.[12] In addition, self-focusing due to plasma heating and relativistic effects have been analyzed with all of these methods. As a rule, these steady-state analyses have predicted stable and periodic propagation of the laser beam in homogeneous plasmas.

It is not clear how such stable self-focusing behavior is established during the transient regime, nor is it clear on what time scales state is achieved. The behavior of the light propagation before steady state occurs, or transient self-focusing, is a subject that merits more investigation. In transient self-focusing, the plasma is not in equilibrium with the pulse, and the character of the focusing changes as the interaction progresses. Because laser pulses are often comparable to or shorter than the hydrodynamic response time of the plasma (which determines the nonlinearity response time in all cases except the relativistic nonlinearity), this is a relevant topic.

Transient self-focusing has been previously analyzed with the paraxial ray method.[13,14] However, as in the steady state case, this method overemphasizes the near-axis influences and ignores the important off-axis effects[12] (as we shall see, these off-axis factors are particularly relevant to transient self-focusing). More rigorous analysis can be performed with a numerical study but this requires huge amounts of computer time and storage for the transient problem.[15,16] Recently, a numerical treatment of laser pulse propagation in plasma with both pondermotive and relativistic nonlinearities was performed.[17] This type of study is difficult to generalize to other situations or regimes, however.

The analysis here seeks to improve upon the paraxial ray method without sacrificing the generality and applicability of the approach as a full numerical study would. We

 0021-8979/83/063003-09$02.40

extend the moment method approach to consider the transient propagation of laser pulses in plasmas due to the ponderomotive and heating nonlinearities. This method is then used as the basis of a simpler numerical treatment that investigates the qualitative features of transient self-focusing. In addition, the method allows analytic investigation of the transient focusing. In particular, we find expressions for the scalings and thresholds of each focusing mechanism. Finally, we find that the off-axis variations of the dielectric constant (not accounted for in previous paraxial studies) may give rise to breakup or futher filamentation of the laser pulse.

The analysis begins in Sec. II with the development of the moment method description of transient propagation of laser pulses in nonlinear media. To utilize this description, the Gaussian ansatz for the pulse radial distribution is assumed and simplified equations describing the radius of the pulse result.

In Sec. III, the plasma response to the laser pulse is derived. This derivation is performed in the context of modeling a particular experiment conducted at the University of Michigan.[18] Briefly, a CO_2 laser pulse was focused into a Helium z-pinch plasma characterized by $T_e \simeq T_i \simeq 20$ eV, and $n_e = 5\times 10^{18}$ cm^{-3}. The laser pulse (without self-focusing) attained an intensity of 10^{11}–10^{12} W/cm^2 in a 125-μm diameter focal spot. Particulars of the experimental set up and plasma target have been previously published.[19–22] The laser pulse duration of 4 nsec is comparable to the plasma hydrodynamic time of 2 nsec (the time during which a sound wave propagates across the laser focal spot). Of particular relevance to this experiment are dielectric constant variations that arise from the electromagnetic field's ponderomotive force and the inverse bremsstrahlung heating. These two mechanisms are analysed in detail in this section.

The results of Sec. II and III are joined for analysis in Sec. IV, and both the analytic and numerical results are presented and discussed there.

II. THE LASER PULSE PROPAGATION

The electric field of the electromagnetic wave in the plasma is governed by the wave equation

$$\nabla^2\mathbf{E} - \nabla(\nabla\cdot\mathbf{E}) - \frac{1}{c^2}\frac{\partial^2}{\partial t^2}\mathbf{E} = \frac{4\pi}{c^2}\frac{\partial}{\partial t}\mathbf{J}. \tag{1}$$

The second term on the left hand side can be ignored if $\nabla(\mathbf{E}\cdot\nabla\epsilon/\epsilon) \ll k_0^2\,\mathbf{E}$, where k_0 is the electric field wave vector and ϵ is the dielectric constant of the plasma. This will be valid if $\nabla_\perp(\nabla_\perp\epsilon/\epsilon) \ll k_0^2$, i.e., the transverse gradient of the dielectric is small compared to the laser wavelength. This implies that either the transverse dielectric variation is weak, or that the plasma is significantly underdense. We assume that this term can be ignored. The current density on the right side of Eq. (1) is derived from the high frequency motion of the electrons,

$$\frac{\partial}{\partial t}\mathbf{J} = -en_e\frac{\partial}{\partial t}\mathbf{v}_e = \frac{\omega_p^2}{4\pi}\mathbf{E}. \tag{2}$$

Equation (1) now becomes the scalar wave equation

$$\nabla^2\mathbf{E} - \frac{1}{c^2}\frac{\partial}{\partial t^2}\mathbf{E} = \frac{\omega_p^2}{c^2}\mathbf{E}. \tag{3}$$

Since we are concerned with the slow time and space variations of the pulse, we will separate them from the high frequency time and space behavior by the substitution

$$E = \tilde{\psi}(\mathbf{x},t)\exp[i(k_0 z - \omega_0 t)] + \text{c.c.}, \tag{4}$$

where k_0 and ω_0 obey the dispersion relation in the undisturbed plasma, $k_0 = \omega_0\epsilon_0^{1/2}/c$, and $\tilde{\psi}(\mathbf{x},t)$ is the pulse envelope. This transforms Eq. (3) into the form

$$2i\left(k_0\frac{\partial\tilde{\psi}}{\partial z} - \frac{\omega_0}{c^2}\frac{\partial\tilde{\psi}}{\partial t}\right) = \Delta_\perp\tilde{\psi} - \frac{\omega_0^2}{c^2}(\epsilon-\epsilon_0)\tilde{\psi} \tag{5a}$$

and

$$-2i\left(k_0\frac{\partial\tilde{\psi}^*}{\partial z} - \frac{\omega_0}{c^2}\frac{\partial\tilde{\psi}}{\partial t}\right) = \Delta_\perp\tilde{\psi}^* - \frac{\omega_0^2}{c^2}(\epsilon-\epsilon_0)\tilde{\psi}, \tag{5b}$$

where we have used the slowly varying envelope approximation (SVEA), which requires that $\partial^2\tilde{\psi}/\partial z^2 \ll k_0^2$ and $\partial^2\tilde{\psi}/\partial t^2 \ll \omega_0^2\tilde{\psi}$. Equations (5) can be cast into a simpler form through a few mathematical manipulations. First, nondimensionalize the independent variables: $z' = k_0 z/\epsilon_0$, $r' = \omega_0 r/c$, and $t' = \omega_0 t$. Then transform Eqs. (5) to the pulse frame with the variable transform $\zeta = z' - t'$, $\tau = t'$. Finally, the imaginary part of the dielectric constant is removed through the transformation $\tilde{\psi} = \psi\exp(-\frac{1}{2}\int^\tau d\tau\,\epsilon_i)$, where ϵ_i is the imaginary part of the dielectric constant. The nonlinear part of ϵ_i is assumed negligible. These operations transform Eqs. (5) into a canonical form of the parabolic wave (or quasi-optic) equations,

$$2i\frac{\partial}{\partial\tau}\psi = \Delta_\perp\psi + f\psi, \tag{6a}$$

$$-2i\frac{\partial}{\partial\tau}\psi^* = \Delta_\perp\psi^* + f\psi^*, \tag{6b}$$

where $f \equiv \epsilon_r - \epsilon_0$ is the nonlinear induced dielectric variation. This is of the same form as the nonlinear Schrödinger equation (NLSE), which has been widely studied in recent years. It differs somewhat from the normal interpretation of the NLSE, because the nonlinear potential f is explicitly dependent upon the variable τ as well as the local field intensity $|\psi|^2$.

Equations. (6) have two invariants. These constants of the motion are

$$I_1 = \int\int dxdy\psi^*\psi, \tag{7}$$

$$I_2 = \int\int dxdy\left(|\nabla_\perp\psi|^2 - \int^\tau d\tau' f\frac{\partial}{\partial\tau'}|\psi|^2\right). \tag{8}$$

The first invariant is merely a statement of the conservation of the pulse energy. The second invariant relates the phase front curvature of the pulse to the plasma nonlinearity.

These two invariants can be used to construct an equation governing the radius of the pulse distribution, which is a measure of the self-focusing. Define the pulse radius $a(\tau)$ as the square root of the second moment of the pulse radial distribution $\langle a^2(\tau)\rangle = \int dA_\perp r^2|\psi|^2/\int dA_\perp|\psi|^2$, where $dA_\perp$ is the differential transverse area. Then using Eqs. (6)–(8), we find the following relation:

$$\frac{d^2}{d^2}\langle a^2(\tau)\rangle = \frac{2I_2}{I_1} - \frac{2}{I_1}\int dA_\perp\left(\frac{r}{2}f\nabla_\perp|\psi|^2 + f|\psi|^2 - \int^\tau d\tau' f\frac{\partial}{\partial\tau'}|\psi|^2\right). \quad (9)$$

Equation (9) allows us to predict the behavior of the pulse radius $a(\tau)$, knowing just the nonlinear potential and the pulse intensity. The nonlinear potential, i.e., the induced dielectric constant change, is determined by the nature of the response of the plasma to the laser pulse. We shall discuss this in the next section. Aside from a knowledge of f, we will also need a relation between $a^2(\tau)$ and $|\psi(r,\tau)|^2$. Postulating a unique relation between the pulse radius and the intensity distribution is equivalent to assuming that the distribution has a constant radial shape. However, this can be a reasonable approximation for many cases of interest.

It is known, for instance, that a pulse with a Gaussian radial profile at $\tau = 0$ will propagate in the shape of a Gaussian if the nonlinear potential is quadratic in r: $f = f_0(\tau) + f'(\tau)r^2$.[23] It has also been shown that for self-trapped light beams [$a(\tau)$ = constant] in plasmas under the influence of a ponderomotive force, the radial shape is approximately an Airy function.[24] The Airy function has a central peak that contains most of the pulse energy, and is well approximated by the Gaussian function in this region. Therefore, we shall assume the pulse intensity to vary as

$$|\psi(r,\tau,\zeta)|^2 = \psi_0^2\frac{a_0^2}{a^2(\tau)}s(\zeta)\exp[-r^2/a^2(\tau)]. \quad (10)$$

This ansatz allows the radius to change under the action of Eq. (9), and ensures that the power is conserved as the radius changes. The function $s(\zeta)$ in Eq. (10) is a form factor, or the envelope shape, of the pulse; its magnitude varies between zero and unity.

Using Eq. (10) in Eq. (9) and performing the radial integrations results in a simplified form for the governing equation:

$$\frac{d^2}{d\tau^2}a^2(\tau) = \frac{2}{a_0^2} - J - 2\int^\tau d\tau'\frac{J}{a}\frac{\partial}{\partial\tau'}a(\tau'), \quad (11)$$

$$J = -\int_0^\infty dr\, r\exp[-r^2/a^2(\tau)]\Delta_r f. \quad (12)$$

III. THE PLASMA RESPONSE

There are a variety of mechanisms in a plasma which can result in the dielectric constant being altered by the laser pulse. We are concerned here only with the change in ϵ due to plasma heating and the ponderomotive force. These processes cause the plasma density to be decreased in the interaction region, altering the nonlinear potential through the relation

$$f = \epsilon_r - \epsilon_0 = \frac{\omega_{p_0}^2}{\omega_0^2}\left(\frac{n_0 - n}{n_0}\right). \quad (13)$$

To study the self-focusing process, we must therefore investigate the response of the plasma density to the laser pulse.

We assume that the Debye length is much smaller than the characteristic scale lengths of the interaction (i.e., the plasma is quasi-neutral) and use a two temperature fluid model. The equations of continuity and momentum are

$$\frac{\partial}{\partial t}n + \nabla\cdot(n\mathbf{u}) = 0 \quad (14)$$

$$\frac{\partial}{\partial t}\mathbf{u} + (\mathbf{u}\cdot\nabla)\mathbf{u} = -\frac{1}{mn_i}\nabla\times[nk_b(ZT_e + T_i)] - \frac{e^2}{4m_e m_i\omega_0^2}\nabla|\psi|^2. \quad (15)$$

These equations have been averaged over the high frequency time variation of the electromagnetic pulse so that only the slow time variations remain. Thus the effect of the laser pulse fields is manifested in the ponderomotive force term on the right hand side of Eq. (15). Linearizing these equations in the variable $\mathbf{u}$, combining, and neglecting the second-order $\nabla T\cdot\nabla n$ term, we obtain

$$\left(\frac{\partial^2}{\partial t^2} - C_s^2\Delta\right)\ln\frac{n}{n_0} = \frac{k_b}{m_i}\Delta(ZT_e + T_i) + \frac{e^2}{4m_e m_i\omega_0^2}\Delta|\psi|^2, \quad (16)$$

where $C_s = [k_b(ZT_e + T_i)/m_i]^{1/2}$ is the ion acoustic wave speed. This is the ion acoustic wave equation, driven by temperature and laser intensity gradients, respectively. Thus, the plasma density, or the nonlinear potential in Eq. (13), will obey an inertial-type time dependent differential equation. This can be contrasted to the more extensively studied diffusive type of nonlinearity,[2] in which the transient nonlinearity is governed by a diffusion type equation.

The temperature gradient that drives the wave equation (16) is found by considering the energy balance equations for the ions and the electrons. They both obey equations of the form

$$\frac{3}{2}n_l k_b\frac{\partial}{\partial t}T = -\nabla\cdot\kappa_l\nabla k_b T_l - \frac{m_e}{m_i}\times\nu_{ei}n_l k_b(T_l - T_k) + |\mathbf{j}_l\cdot\mathbf{E}|, \quad (17)$$

where the subscript l denotes electrons or ions and the subscript k denotes ions or electrons, respectively. This energy balance accounts for temperature change due to thermal conduction losses, collisional losses/gains, and Joule heating (inverse bremsstrahlung). The heating term is a result of the high frequency part of the electric field acting upon the part of the induced current that is in phase with the field (due to collisional drag on the oscillating particle). The induced current is

$$\mathbf{j}_l = -en_l\mathbf{v}_l = \frac{e^2n_l\mathbf{E}}{m_l(\omega_0^2 + \nu_{ei}^2)}(\nu_{ei} - i\omega_0), \quad (18)$$

which gives rise to the heating term:

$$\mathbf{j}_l\cdot\mathbf{E} = \frac{\omega_p^2\nu_{ei}}{4\pi\omega_0^2}|\psi|^2. \quad (19)$$

We have assumed $\nu_{ei} \ll \omega_0^2$. It can be immediately seen that the electrons, because of their much smaller mass, are heated much more strongly than the ions. The only other source of ion heating occurs via collisions with electrons, in the second term of Eq. (17) for the ions. The important parameter affect-

ing this energy transfer is the electron–ion energy equilibration time, $\tau_{ei} = m_i/m_e\ \nu_{ei}$. In the experiment under investigation here, this energy equilibration time is initially 5 nsec, on the same order as the total interaction time. However, as the plasma rapidly heats, τ_{ei} (varying as $T_e^{-3/2}$) increases quickly to an order of magnitude larger, so that the ions gain relatively little energy from the electrons in the time of interest. Thus, we ignore the ion energy balance equation, and assume the ion temperature to be constant. This leaves only the electron energy balance.

Depending upon the state of the plasma, either electron–ion collisions or thermal conduction will play the dominant role in transferring energy away from the heated electrons in the interaction region. The ratio of the conduction loss to the collisional loss is given by the parameter $R = m_i\, v_{Te}^2/m_e\, a_0^2\, \nu_{ei}^2$, where $v_{Te} = (k_b\, T_e/m_e)^{1/2}$ is the electron thermal speed. If $R \gg 1$, the electrons escape from the heated region before they lose appreciable energy in collisions with ions, and conduction losses will be dominant. In the CO_2 laser-plasma experiment under consideration, $R \simeq 10$ before the plasma is significantly heated, and increases rapidly (as T_e^4) as heating occurs. It is therefore quite reasonable to ignore the collisional loss term in comparison to the conduction losses.

Now consider the effect of the time derivative term on the left hand side of Eq. (17). In the presence of conduction losses, the equilibration time for the temperature distribution is determined by the characteristic time $t_{eq} = r^2 n_e/\kappa_e$. This equilibration time is dependent upon the distance r from the heating source. Since it takes a finite time for a temperature disturbance to propagate from its point of origin to any given distance, the temperature gradient at small radii equilibrates quickly, whereas at some radius $r_{eq} = (\kappa_e\ t/n_e)^{1/2}$, the temperature is still changing. At arbitrarily large times, there are always some distant points still undergoing some temperature change. Since the temperature magnitude at all points is dependent upon the magnitude at these distant points (through boundary conditions), the absolute temperature never equilibrates. Only the gradients at points $r < r_{eq}$ will equilibrate.

To illustrate this behavior clearly, consider the following simple model of the laser beam heating. The heating gives rise to a cylindrical heat source of radius a_0 in the plasma, emitting a (constant) heat flux of magnitude q_0 given by $q_0 = \int_0^\infty dr\, r\, (\omega_p^2\ \nu_{ei}\ |\psi|^2/4\pi\omega_0^2\ k_b a_0)$. The temperature distribution resulting from this situation is known to be[25] (for $r > a_0$)

$$T_e(r,t) = T_{e0} + \int_0^\infty du(1 - \exp[-2\kappa_e t u^2/3n_e)] \times \left(\frac{J_0(ur)Y_1(ua_0) - Y_0(ur)J_1(ua_0)}{u^2[J_1^2(ua_0) + Y_1^2(ua_0)]}\right)\frac{2q_0}{\pi\kappa_e}. \quad (20)$$

where $J_\alpha(x)$ and $Y_\alpha(x)$ are Bessel functions of the first and second kind of order α. This solution exhibits two important characteristics. First, it is known that for large times ($t \gg t_{eq}$), the solution behaves in the asymptotic manner

$$T_e(r,t) = T_{e0} + \frac{q_0 a_0}{2\kappa_e}\ln\left(1.46\,\frac{\kappa_e t}{n_e r^2}\right) + O(t_{eq}/t). \quad (21)$$

Secondly, this shows that the asymptotic solution depends only upon the characteristic relaxation time t_{eq} that we found previously. Note that the temperature at any point increases monotonically to infinity; no equilibrium is found. However, the spatial derivatives of the temperature distribution do equilibrate for times $t/t_{eq} \gg 1$, behaving as:

$$\nabla_r^n\, T_e(r,t) = \text{constant} \times r^{-n} + O(t_{eq}/t). \quad (22)$$

Thus, for $t/t_{eq} \gg 1$, the temperature gradients and the temperature magnitude become uncoupled; the gradients equilibrate and the magnitude does not.

In the formulation here, we are concerned primarily with the temperature gradients in the light propagation region, $r \leqslant a$. The equilibration time in this region ($\sim 100\,\mu$m across) is much smaller than the characteristic variation time of the laser pulse envelope: $t_{eq} \simeq 100$ psec, and $t_p = 4$ nsec. In addition, this equilibration time decreases rapidly as the plasma is heated, since $t_{eq} \propto T_e^{-5/2}$. Thus, the temperature gradients in the interaction region can be considered to be in instantaneous equilibrium with the inverse bremsstrahlung heating:

$$k_b \nabla\cdot\kappa_e \nabla T_e = \omega_p^2\ \nu_{ei}\,|\psi|^2/4\pi\omega_0^2. \quad (23)$$

In contrast, the temperature magnitude in this region (upon which the coefficients κ_e, ν_{ei}, and C_s depend parametrically) must be found through solution of the full nonlinear time dependent temperature balance equation

$$\frac{3}{2} n_e k_b \frac{\partial}{\partial t} T_e = -\nabla\cdot\kappa_e \nabla k_b T_e + \frac{\omega_p^2\ \nu_{ei}}{4\pi\omega_0^2}\,|\psi|^2 \quad (24)$$

Equation (23) can be directly substituted into the wave equation (16) if the temperature dependence of the conductivity coefficient ($\kappa_e \propto T_e^{5/2}$) can be ignored in the region $r \leqslant a$. This requires the temperature change across the pulse region to be small, which can occur if the plasma heating is either very small or very large. This condition can be quantified by solving Eq. (23) in the following manner: approximate the collision frequency as constant, evaluated at the temperature T_e ($r = a, t$) (this slightly overestimates the heating and thus gives a small overestimate of the resulting change). Integrate Eq. (23) using $\kappa_e = \kappa_{e0}\ T_e(r,t)^{5/2}$ and $\nu_{ei} = \nu_{ei0}\ T_e(a,t)^{-3/2}$; in terms of the boundary temperature $T_e(a,t)$ and the pulse power ψ^2, one finds

$$T_e(r,t) = T_e(a,t)\left\{1 + \frac{7\omega_p^2 \nu_{ei0}\ \psi^2 a_0^2}{32\pi\omega_0^2 k_b \kappa_{e0}\ T_e(a,t)^{7/2}} \times\left[\text{Ei}(1) - \text{Ei}\left(\frac{r^2}{a^2}\right)\right]\right\}^{2/7}, \quad (25)$$

where $\text{Ei}(z) = \int_0^z dt\,[1 - \exp(-t)]/t$ is the Exponential integral.[26] In order that the temperature difference satisfy the condition $[T_e(r=0,t) - T_e(a,t)]/T_e(a,t) \ll 1$, the boundary temperature $T_e(a,t)$ must obey the relation:

$$2\times 10^{-39}\lambda^2(\mu\text{m}) n_e^2(\text{cm}^{-3}) P(\text{Watts})/\xi_0^{1/2} \ll T_e^5(a,t)(\text{eV}). \quad (26)$$

This will be satisfied if the heating is weak (the power P is small) of if the heating is strong (the boundary temperature is large). If this inequality is validated, Eq. (23) can be linearized and directly substituted into Eq. (16) to yield

$$\left(\frac{\partial^2}{\partial t^2} - C_s^2\Delta\right)\ln(n/n_0) = -\beta|\psi|^2 + \alpha\Delta|\psi|^2, \quad (27)$$

where $\beta = \omega_{pe}^2 \nu_{ei}/4\pi m_i \kappa_e \omega_0^2$ and $\alpha = e^2/4m_e m_i \omega_0^2$. Eq. (27), along with the pulse radius governing Eq. (11), forms the basis of this study of transient self-focusing. The complete temperature balance Eq. (24) is an auxiliary equation that affects the basic set Eqs. (11) and (27) parametrically.

IV. ANALYSIS

A. Threshold determination

The self-focusing threshold is given by the self-trapped propagation condition. The pulse is self-trapped when the radius remains constant and the pulse neither diffracts nor focuses. This occurs when the first two terms on the right hand side of Eq. (11) cancel each other, $J = 2/a_0$, and the pulse enters the plasma with $da/d\tau = 0$. When self-trapping occurs, the density change in the propagation region is small, and we can linearize the wave equation (27) in the density by expanding the logarithm. J can then be found through integral transform techniques; the result is

$$J = \frac{\omega_{p0}^2 \psi_0^2 a_0^2 a(\tau)}{\epsilon_0 \omega_0 c_s^4} \int_0^\infty du \frac{s(\tau - u)}{\tau_r'^3} \left(\beta \frac{d}{dx}[xD(x)]\Big|_{x = u/\tau_r'} + \frac{2\alpha}{c_s^2 \tau_r^2} \frac{d}{dx}(x^2 + [3x - 2x^3)D(x)]\Big|_{x = u/\tau_r'}, \quad (28)$$

where $\tau_r' = [a^2(\tau) + a^2(\tau - u)C_s^2]^{1/2}$, and $D(x) = \exp(-x^2)\int_0^x dt \exp(-t^2)$ is Dawson's integral.[26] We have assumed for convenience that the change in C_s due to plasma heating is negligible. Next, assuming that the radius of the pulse has experienced little change previous to self-trapping, we can replace $a(\tau)$ by a_0, the characteristic pulse radius in the trapped region. Then taking the pulse envelope shape to be a step function [$s(t) = 1$ for $t \geqslant 1$; $= 0$ otherwise], the integral in Eq. (28) can be analytically performed to yield.

$$J = \frac{\omega_{p0}^2 \psi_0^2}{2\epsilon_0 \omega_0^2 C_0^2}\{s_0^2 \beta \check{t} D(\check{t}) + [\check{t}^2 + (3\check{t} - 2\check{t}^3)D(\check{t})]\}, \quad (29)$$

where $\check{t} = t/\tau_r = tC_s/\sqrt{2}a_0$. This can now be used, along with the self-trapped condition, to determine the power necessary to achieve self-trapping at the time $\check{t}$. We find these threshold powers to be

$$P^T(\check{t}) = P_{ss}^T/2\check{t}D(\check{t}), \quad (30a)$$

$$P^P(\check{t}) = P_{ss}^P/[\check{t}^2 + (3\check{t} + 2\check{t}^3)D(\check{t})], \quad (30b)$$

for the thermal heating and the ponderomotive force mechanisms, respectively. P_{ss}^T and P_{ss}^P are the corresponding steady-state power thresholds.

$$P_{ss}^T = 2\pi\epsilon_0^{1/2} C_s^2 c^3 m_i \kappa_e \omega_0^2/a_0^2 \nu_{ei} \omega_p^4, \quad (31a)$$

$$P_{ss}^P = 2\epsilon_0^{1/2} C_s^2 c^3 m_i m_e \omega_0^2/e^2 \omega_p^2, \quad (31b)$$

The transient thresholds [Eq. (30)] are shown in Fig. 1. Self-focusing is thus possible for $t \ll 1$, if the power levels are sufficiently far above threshold.

Also, note the extreme temperature dependence of the thermal self-focusing threshold, which varies as T_e^5. Since this mechanism is responsible for heating the plasma, it will saturate and turn itself off as the temperature in the interaction region rises. Since there is no equilibrium temperature, we conclude that thermal self-focusing has no true steady state existence; it is inherently a transient phenomenon.

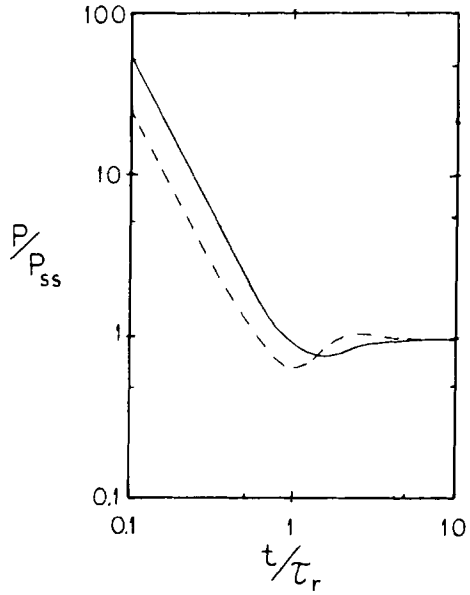

FIG. 1. Transient self-focusing power thresholds as a function of the interaction time, $\tau_r = 2a_0/C_s$, and the steady-state power thresholds P_{ss} are given by Eq. (28) in the text. The solid line corresponds to the thermal mechanism, the dashed line corresponds to the ponderomotive mechanism.

B. Numerical analysis

To illustrate the transient self focusing process and study the propagation of the pulse, Eqs. (11), (24), and (27) were numerically solved (details appear in the Appendix). The parameters used as input for these calculations correspond to the experiment described previously,[18] except that the pulse length used in the calculations is 1.5 nsec instead of 4 nsec. The change in pulse radius due to the self-focusing is shown in Fig. 2, for a pulse power of 6.5×10^{11}/W/cm^2.

The peak pulse power in this simulation is initially far above threshold for both mechanisms: 1.3×10^4 times the steady-state thermal threshold and 13 times the steady-state ponderomotive threshold, evaluated at the initial conditions ($T_e = T_i = 20$ eV). However, the plasma is very rapidly heated from classical inverse bremsstrahlung (see Fig. 3). The plasma heating increases the threshold power levels of the mechanisms, especially in the case of the thermal self-focusing process. At the pulse peak the power is only just above the ponderomotive threshold and below the thermal threshold, as shown in Fig. 4. Although the thermal mechanism is quite dominant at the low initial temperature, the rapid heating reduces the power below threshold and the ponderomotive force becomes the dominant self-focusing mechanism.

The qualitative behavior of the pulse propagation is also of interest. After quickly self-trapping, the pulse forms one and successively more focal spots, which move upstream. After a short while, the pulse forms only a single tight focus, and the other foci are lost in the large diffraction of this post

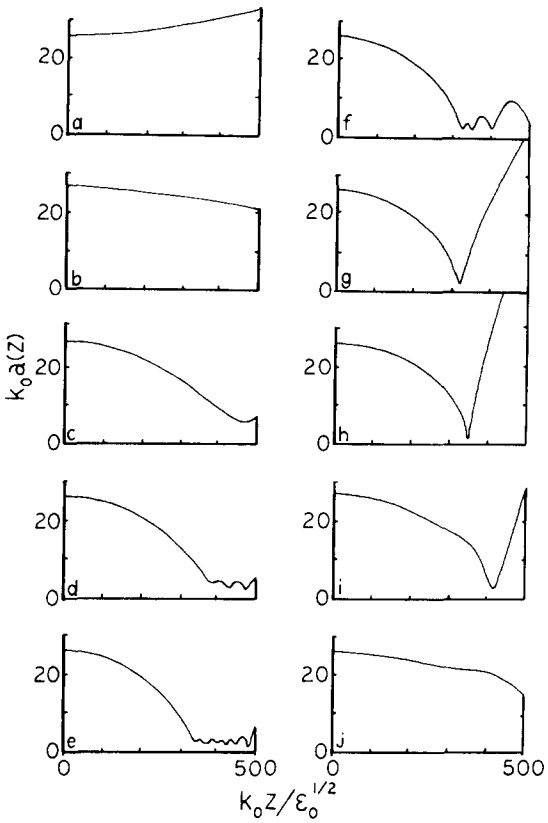

FIG. 2. Variation of the pulse radius in the plasma at different times during the interaction. (a) $t = 0$; (b) $t = 0.14\tau_p$; (c) $t = 0.27\tau_p$; (d) $t = 0.34\tau_p$; (e) $t = 0.41\tau_p$; (f) $t = 0.48\tau_p$; (g) $t = 0.54\tau_p$; (h) $t = 0.68\tau_p$; (i) $t = 0.82\tau_p$; (j) $t = 0.95\tau_p$.

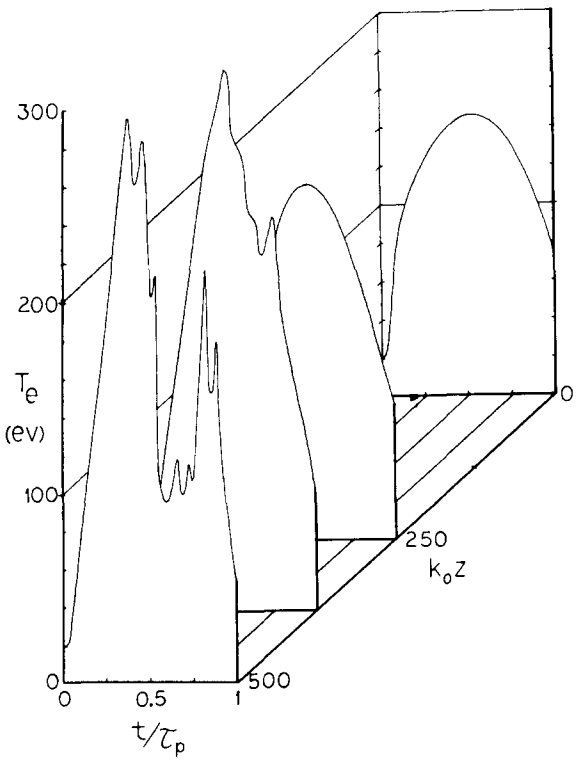

FIG. 3. Average pulse region electron temperature vs time, at different points in the plasma.

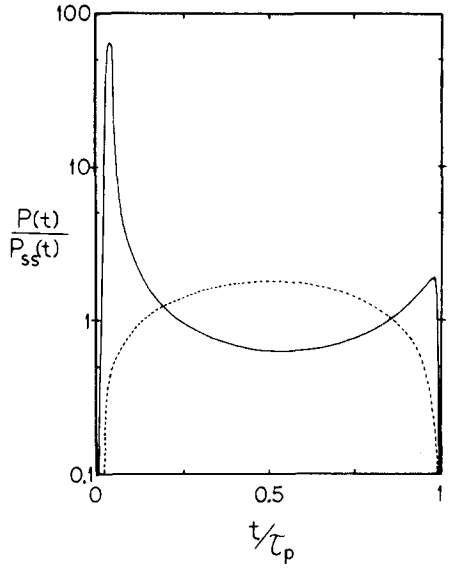

FIG. 4. Laser pulse power at $z = 0$ vs time, normalized to the steady-state self-focusing threshold powers, P_{ss}. P_{ss} changes in time due to the changing electron temperature. The solid line is the pulse power normalized to the thermal threshold, the dotted line is normalized to the ponderomotive threshold.

focal region. The large angle this diffracted light forms with the centerline may explain some of the anomalous decrease in energy transmission observed in some experiments, when the incident power level is raised.[18,22,27] Only the light in a relatively small angle of the forward direction is captured by the detection apparatus, so transmitted light at larger angles escapes detection. Since the angle of this diverted light increases as the focal spot size decreases, the energy collected and measured will decrease as the pulse power (or self-focusing) increases.

This decrease of (detected) transmitted energy with increasing input energy has been calculated in the numerical analysis, and the results are shown in Fig. 5. The calculation

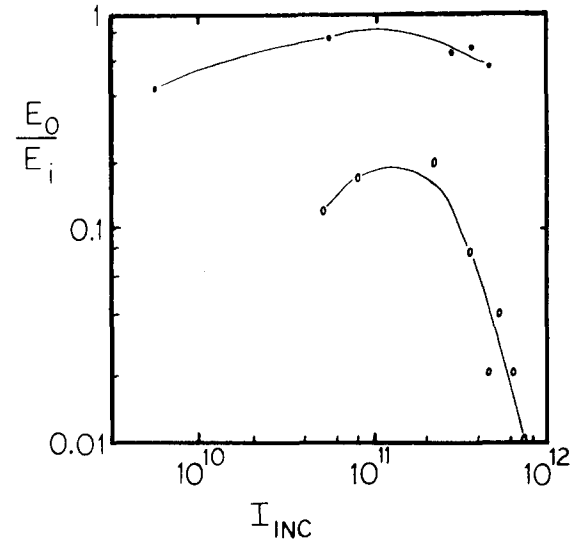

FIG. 5. Total transmitted energy fraction (detected in a 14° forward angle) vs incident power. Solid dots are computational results; open dots are experimental results.

agrees with the qualitative behavior of the experimental curve,[18] as well as approximating the correct turning point at about $I_{inc} = 10^{11}$W/cm^2. [The energy fraction increases with incident power in the lower power regime because the average plasma temperature increases and the absorption ($\sim T_e^{-3/2}$) decreases.] However the calculation consistently predicts higher transmission levels at all powers. This may be due to several other nonlinear mechanisms that can be present with the higher intensities produced in the self-focused regions. For instance, parametric instabilities such as stimulated Brillouin scattering can either scatter light out of the detection angle or cause increased absorption of the light by the plasma. The modeling here does not include these competing effects.

The transition of the propagation behavior from periodic focusing, Fig. 2(e), to the singular focus/large diffraction behavior, Fig. 2(g), can be explained by studying the details of the plasma density dynamics. Figure 6 shows the density distribution changing in time at different points along the propagation path. The action of the moving focal spots creates ion acoustic waves in the pulse region which propagate radially outward. Each time a focus passes a given point, it provides an impulse at the centerline which produces another wave. The wavelength of the ion acoustic wave is approximately equal to the focal spot size. These waves cause a net diffractive effect on the Gaussian pulse propagating through this region.

The moment method approach fails in this region. Since the density distribution in the propagation area is no longer close to quadratic, distortion of the pulse from the Gaussian profile ansatz is expected to be significant. The wave troughs act as separate lenses, and one expects that the pulse would break up radially into discrete, separate sections. In this way, the filamentation of the pulse may begin. Some evidence of radial breakup in numerical simulations (that allowed for pulse distortion) has been seen before.[17] However, the results of that simulation are not relevant here, since the time scales considered were very small ($\tau_p/\tau_r \ll 1$, so that the wave troughs had no chance to form) and the nontransient relativistic nonlinearity played a dominant role.

It is interesting to speculate how these ion acoustic waves will interact with the filamenting pulse on a longer time scale. After the waves propagate from the interaction region, will the density in the region remain oscillatory (and the pulse remain filamented), or will the density distribution smooth out and reduce or stop the filamentation? To fully study the transition from transient to steady state, the Gaussian ansatz assumption must be discarded and an analysis which allows for changes in the radial shape of the pulse must be performed. Such a self-consistent description of the pulse distortion is currently being investigated.

V. SUMMARY

The moment method has been used to investigate transient self-focusing in plasmas induced by thermal and ponderomotive forces. Previous analyses of the phenomenon have utilized the paraxial ray method, which confines its description of the pulse to areas very close to the propagation axis. In contrast, the moment method accounts for the effect of the off-axis nonlinearity on the pulse mean radius. However, since the Gaussian shape ansatz has been used to characterize the pulse, transverse distortion or breakup of the pulse is not taken into account.

Analytic expressions for the transient power threshold are found, and we show that self focusing is possible for times much smaller than the characteristic plasma response time. In addition, the scaling of the threshold powers reveals that the thermal self-focusing mechanism rapidly decreases as the temperature rises due to plasma heating. Since the temperature in the interaction region never equilibrates (contrary to previous assumptions), the thermal self-focusing process is inherently a transient phenomenon.

Numerical integration of the governing equation for the pulse radius, using the Gaussian ansatz, reveals the nature of the propagation of the laser pulse. As in other analyses, we find that the laser pulse forms several focal spots which proceed to move upstream along the pulse axis. This action generates ion acoustic waves that propagate radially outward, causing a net diffractive effect on the pulse in this model. If the Gaussian ansatz were discarded, we would expect that these ion acoustic waves will cause transverse breakup of the pulse, or further filamentation. This breakup mechanism may be entirely transient, or it may have lasting effects that alter the expected steady state pulse propagation. In order to determine this, the Gaussian ansatz must be discarded and the pulse must be allowed to freely distort in shape.

Finally, we note that this analysis excludes other nonlinear plasma phenomena that often accompany self-focusing. The primary effect of these generated instabilities would be to increase the absorption or scattering of the pulse as it propagates, decreasing the power levels further into the plasma, but not altering the qualitative behavior noted here. The large amplitude plasma modes caused by such processes, like the ion acoustic waves generated by the moving foci, may also generate a turbulent state in the plasma. Besides altering the absorption and scattering levels as noted before, the turbulence will also increase the net diffractive force felt by the pulse.[28]

ACKNOWLEDGMENT

This work was partially supported by Grant AFOSR-80-0029.

APPENDIX: NUMERICAL SOLUTION OF THE SELF-FOCUSING EQUATIONS

The self focusing problem is numerically analysed by solving the main governing equations: the pulse radius governing Eq. (11); the density wave Eq. (27); and the electron temperature Eq. (24). The pulse and the plasma are broken up into meshes in the ζ and z directions, respectively, and the equations are solved as the ζ mesh propagates through the z mesh one mesh point at a time.

A. The pulse radius governing equation

A perturbation solution to Eq. (11) is used to propagate the pulse radius over small distances, and is repeatedly ap-

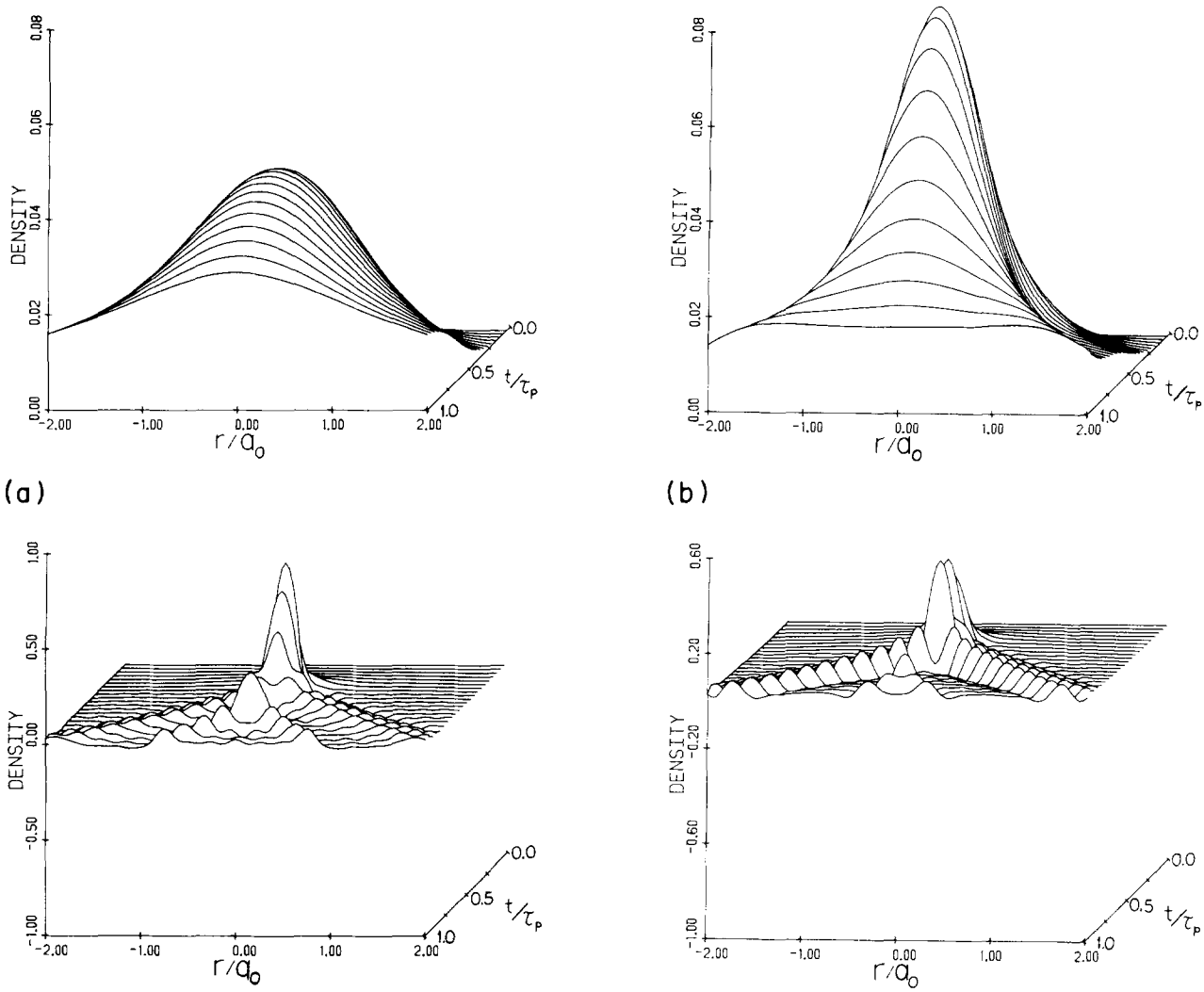

FIG. 6. Plasma density vs time and radius at different points in the plasma; vertical axis is the negative density change $(n - n_0)/n_0$. (a) $k_0 z = 0$; (b) $k_0 z = 250$; (c) $k_0 z = 375$; (d) $k_0 z = 500$. Parameters are the same as Fig. 1.

plied to follow the pulse points as they pass through the plasma. First Eq. (11) is transferred to the z frame. Denoting the z mesh points by the subscript i and the ζ mesh points by the index m, we can follow a particular pulse point m as it propagates to the z mesh point i by

$$\frac{d^2}{dz^2} a^2(z_i,t_{im}) = \frac{2}{a_0^2} - J(z_i,t_{im}) - 2\int_0^{z_i} dz' \times \frac{J(z',t'_m)}{a(z',t'_m)} \frac{da(z',t'_m)}{dz'} \quad \text{(A1)}$$

where $t'_m = z' - \zeta_m$ and $t_{im} = z_i - \zeta_m$ are the times at which the pulse point at ζ_m reaches the points z' or z_i in the plasma. The values of J are defined and calculated at the points (z_i,t_{im}) and are linearly interpolated in between

$$J(z,t_m) = J(z_i,t_{im}) + \frac{(z - z_i)}{(z_{i+1} - z_i)} \times [J(z_{i+1},t_{i+1,m}) - J(z_i,t_{im})], \quad \text{(A2)}$$

for $z_i \leqslant z \leqslant z_{i+1}$ and $t_m = z - \zeta_m$. Using the form in Eq. (A1), we can find an analytic solution valid for small steps δz:

$$a^2(z_i + \delta z) = (da_i^2/dz + \Delta J_i/\Delta z_i)\sin(J_i^{1/2}\,\delta z/a_i)/(J_i^{1/2}/a_i) + a_i^2[1 - (2/a_0^2 - \mathscr{H}_i)/J_i]\cos(J_i^{1/2}\,\delta z/a_i) + a_i^2(2/a_0^2 - \mathscr{H}_i)/J_i - \Delta J_i a_i \delta z/J_i^{1/2} \quad \text{(A3)}$$

where $\mathscr{H}_i = \int_0^{z_i} dz' J(z',t')d\{\ln[a^2(z')]\}/dz'$; $\Delta J_i = J_{i+1} - J_i$; $\Delta z_i = z_{i+1} - z_i$. Using small step $\delta z \leqslant z_i$ [small enough so that the perturbational approximations made in Eq. (A3) are satisfied], this equation is used to follow the pulse section ζ_m as it passes from z_i to z_{i+1}, $i = 1,2....$

B. Density wave equation

The density wave Eq. (27) is analytically solved in the Hankel transform space; the solution is found to be

$$\ln\frac{n}{n_0}(\xi,z,t_0 + \delta t) = \ln\frac{n}{n_0}(\xi,z,t_0)\cos C_s\,\xi\delta t \times \frac{d}{dt}\left[\ln\frac{n}{n_0}(\xi,z,t_0)\right]\frac{\sin C_s\,\xi\delta t}{C_s t}$$

$$-\int_{t_0}^{t_0+\delta t} dt' \frac{\sin C_s \xi (t-t')}{C_s \xi} [\beta(t') + \alpha \xi^2] \times \exp[-\xi^2 a^2(z,t')/4]. \quad \text{(A4)}$$

After numerical integration of the last term at each time step, this density is numerically inverse Hankel transformed, and then averaged in the manner of Eq. (12) to calculate J.

C. The electron temperature equation

Under the assumption of Eq. (26), the electron temperature in the pulse region is relatively constant in the radial direction, so a single radially averaged temperature is calculated at each point z. Since this temperature enters the calculation in a parametric manner, and doesn't directly influence the self-focusing, it was felt that a reasonable estimate for the temperature would suffice for the calculation. This estimation also eases the calculational and storage requirements of the numerical analysis.

The key approximation is to let the coefficients κ_e and ν_{ei} depend only upon the radially averaged temperture, defined as

$$\langle T_e(t) \rangle = a^{-2}(t) \int_0^\infty dr r \exp[-r^2/a^2(t)] T_e(r,t). \quad \text{(A5)}$$

This formalism allows κ_e and ν_{ei} to vary in time as they should, but constrains them to be spatially constant. The result is an underestimation of the plasma heating, mainly because the conductivity at large distances is at an artificially high level, determined by the electron temperature in the hot region. We can still show, however, that the interaction easily heats the plasma to a high enough level that the thermal self-focusing mechanism (which is the most temperature sensitive process here) becomes negligible.

Utilizing this approximation allow us to solve for the averaged temperature directly

$$\langle T_e \rangle = T_{e0} + \int_0^t du \bar{\omega}_p^2 (t-u) \nu_{ei} \times [\langle T_e(t-u) \rangle, \bar{n}_e(t-u)] \psi_0^2 a_0^2 s(t-u) / \times \{ [12\pi\omega_0^2 \bar{n}_e(t-u) k_b a^2(t-u)] \times \left[a^2(t) + a^2(t-u) + 4 \int_0^u dt' \chi(t') \right] \} \quad \text{(A6)}$$

where $\chi(t)' = 2\kappa_e [\langle T_e(t') \rangle]/3\bar{n}_e(t')$ and

$$\bar{n}_e(t) = \int_0^\infty dr r \exp[-r^2/a^2(t)] n_e(r,t)/a^2(t).$$

[1] M. Hercher, J. Opt. Soc. Am. **54**, 563 (1964).
[2] J. H. Marburger, Prog. Quantum Electron **4**, 35 (1975).
[3] A. B. Langdon and B. F. Lasinski, Phys. Rev. Lett. **34**, 934 (1975).
[4] P. Kaw, G. Schmidt, and T. Wilcox, Phys. Fluids **16**, 1522 (1975).
[5] E. Valeo, Phys. Fluids **17**, 1391 (1974).
[6] E. Valeo and K. Estabrook, Phys. Rev. Lett. **34**, 1008 (1975).
[7] C. Max, J. Arons, and A. B. Langdon, Phys. Rev. Lett. **33**, 209 (1974).
[8] C. Max, Phys. Fluids **19**, 74 (1976).
[9] M. S. Sodha, A. K. Ghatak, and V. K. Tripathi, *Progress in Optics XIII*, edited by E. Wolf (North-Holland, Amsterdam, 1976), p. 169.
[10] J. F. Lam, B. Lippmann, and F. Tappert, Phys. Fluids **20**, 1176 (1977).
[11] D. Anderson and M. Bonnedal, Phys. Fluids **22**, 105 (1979).
[12] D. Subbarao and M. S. Sodha, J. Appl. Phys. **50**, 4604 (1979).
[13] M. S. Sodha, S. Prasad, and V. K. Tripathi, J. Appl. Phys. **46**, 637 (1975).
[14] M. S. Sodha, D. P. Singh, and R. P. Sharma, J. Appl. Phys. **50**, 2678 (1979).
[15] J. A. Fleck, J. A. Morris, and M. D. Feit, Appl. Phys. **10**, 129 (1976).
[16] F. P. Mattar and M. C. Newstein, Comput. Phys. Commun. **20**, 139 (1980).
[17] E. L. Kane and H. Hora, Aust. J. Phys. **34**, 385 (1981).
[18] D. Voss, Ph.D. thesis, University of Michigan, 1981.
[19] D. G. Steel, P. D. Rockett, D. R. Bach, and P. L. Colestock, Rev. Sci. Instrum. **49**, 456 (1978).
[20] D. Duston, P. D. Rockett, D. G. Steel, J. G. Ackenhusen, D. R. Bach, and J. J. Duderstadt, Appl. Phys. Lett. **31**, 801 (1977).
[21] P. D. Rockett, D. G. Steel, J. G. Ackenhusen, and D. R. Bach, Phys. Rev. Lett. **40**, 649 (1978).
[22] J. G. Ackenhusen and D. R. Bach, Appl. Phys. Lett. **34**, 360 (1979).
[23] J. Arnaud, *Beam and Fiber Optics* (Academic, New York, 1976).
[24] F. S. Felber, Phys. Fluids **23**, 1410 (1980).
[25] H. S. Carslaw and J. C. Jaeger, *Conduction of Heat in Solids* (Clarendon, Oxford, 1947).
[26] M. Abramowitz and I. Stegun, editors, *Handbook of Mathematical Functions* (U. S. Government Printing Office, Washington, 1964).
[27] C. Joshi, C. E. Clayton, A. Yasuda, and F. F. Chen, J. Appl. Phys. **53**, 215 (1982).
[28] V. A. Petrishchev, Radiophys. Quant. Electron. **14**, 1112 (1971).